

NACA RM L52F03

NACA

FOR REFERENCE

NOT TO BE TAKEN FROM THIS ROOM

# RESEARCH MEMORANDUM

AERODYNAMIC CHARACTERISTICS AT SUPERSONIC SPEEDS OF A

SERIES OF WING-BODY COMBINATIONS HAVING CAMBERED

WINGS WITH AN ASPECT RATIO OF 3.5

AND A TAPER RATIO OF 0.2

EFFECT AT  $M = 2.01$  OF NACELLE SHAPE AND POSITION ON

THE AERODYNAMIC CHARACTERISTICS IN PITCH

OF TWO WING-BODY COMBINATIONS

WITH  $47^\circ$  SWEEPBACK WINGS

By Cornelius Driver

Langley Aeronautical Laboratory  
Langley Field, Va.

CLASSIFIED DOCUMENT

This material contains information affecting the National Defense of the United States within the meaning of the espionage laws, Title 18, U.S.C., Secs. 793 and 794, the transmission or revelation of which in any manner to an unauthorized person is prohibited by law.

## NATIONAL ADVISORY COMMITTEE FOR AERONAUTICS

WASHINGTON

July 25, 1952

CONFIDENTIAL

CLASSIFICATION CHANGED

UNCLASSIFIED

To

*effective*  
*May 11, 1958*  
Date  
*NACA Res also*  
*VRN-127*  
By authority of  
*AM 16-2-58*



3 1176 01436 4781

NATIONAL ADVISORY COMMITTEE FOR AERONAUTICS

## RESEARCH MEMORANDUM

AERODYNAMIC CHARACTERISTICS AT SUPERSONIC SPEEDS OF A  
SERIES OF WING-BODY COMBINATIONS HAVING CAMBERED  
WINGS WITH AN ASPECT RATIO OF 3.5  
AND A TAPER RATIO OF 0.2  
EFFECT AT  $M = 2.01$  OF NACELLE SHAPE AND POSITION ON  
THE AERODYNAMIC CHARACTERISTICS IN PITCH  
OF TWO WING-BODY COMBINATIONS  
WITH  $47^\circ$  SWEEPBACK WINGS

By Cornelius Driver

## SUMMARY

An investigation at  $M = 2.01$  has been conducted in the Langley 4- by 4-foot supersonic pressure tunnel to determine the effect of a series of nacelles on the longitudinal stability characteristics of a sweptback wing-body combination. Nacelle shape and position were varied on a configuration with a 6-percent-thick wing having an aspect ratio of 3.5, a taper ratio of 0.2, and  $47^\circ$  of sweep at the quarter chord. Simulated partially submerged nacelles were tested on this wing-body combination and also on a similar configuration with a wing having a 12-percent-thick root section. The Reynolds number was  $2.2 \times 10^6$  based on the wing mean aerodynamic chord.

The shape and location of the external nacelles had only small effects on the drag coefficient and the lift-drag ratio of the configurations tested. With the partially submerged nacelle configurations (tested without internal air flow), the total drag was about the same for the 6-percent-thick wing and the wing with thickened root sections. In general, the magnitudes of the drag-coefficient increments at  $M = 2.01$  were of the same order as the drag increments at  $M = 1.6$ .

## INTRODUCTION

A research program has been in progress at the Langley Aeronautical Laboratory to determine at subsonic, transonic, and supersonic speeds the effects of thickness ratio and sweep on the aerodynamic characteristics of a series of wing-body combinations. The cambered wings have an aspect ratio of 3.5 and a taper ratio of 0.2. The effects of sweep at subsonic and transonic speeds are presented in references 1 and 2. The effects of sweep, thickness ratio, and nacelle position on the longitudinal and lateral stability characteristics at a Mach number of 1.60 are presented in references 3, 4, and 5. The effects of both sweep and thickness ratio on the longitudinal and lateral stability characteristics at a Mach number of 2.01 are presented in references 6 and 7.

This paper presents the results of tests at  $M = 2.01$  of a majority of the nacelle configurations previously tested at  $M = 1.60$  (ref. 5). The nacelle shape and location were varied on a 6-percent-thick wing having the quarter-chord line swept back  $47^\circ$ . Simulated submerged nacelles were also tested on this configuration and on a similar configuration with a wing having a thickened root section. The root-section thickness ratio varied linearly from 12 percent at the body center line to 6 percent at the 40-percent-semispan station. Lift, drag, and pitching-moment results are presented for a Mach number of 2.01 and a Reynolds number of  $2.2 \times 10^6$  based on the wing mean aerodynamic chord. The data of this paper are presented with a minimum of analysis to expedite publication.

## SYMBOLS

|              |   |
|--------------|---|
| $\bar{c}$    | mean aerodynamic chord of wing, 0.646 ft  |
| $C_D$        | drag coefficient, $D/qS$  |
| $\Delta C_D$ | nacelle drag increment, drag-coefficient rise due to addition of nacelles to basic wing configuration |
| $C_L$        | lift coefficient, $L/qS$  |
| $C_m$        | pitching-moment coefficient about the quarter chord of the mean aerodynamic chord, $m/qS\bar{c}$      |
| $D$          | drag  |
| $L$          | lift  |

|          |   |
|----------|---|
| M        | Mach number                                   |
| m        | pitching moment                               |
| p        | static pressure                               |
| q        | dynamic pressure, $\frac{\gamma}{2} \rho M^2$ |
| S        | wing-plan-form area, 1.143 sq ft              |
| $\alpha$ | angle of attack, deg                          |
| $\gamma$ | ratio of the specific heats of air            |
| $\psi$   | angle of yaw, deg                             |

#### APPARATUS

##### Tunnel

The tests were conducted in the Langley 4- by 4-foot supersonic pressure tunnel described in reference 3.

##### Models and Equipment

The basic wing-body configuration (fig. 1) consisted of a body formed by an ogival nose and a constant-diameter cylindrical section with a 6-percent-thick tapered wing having the quarter-chord line swept back  $47^\circ$ . Body and wing dimensions are given in figure 1. For one test, the 6-percent-thick wing was replaced by a similar wing with a thickened root section. The thickness of the wing varied linearly from 12 percent at the fuselage center line to 6 percent at the 40-percent-semispan station and was a constant thickness ratio over the remainder of the semispan. Ordinates for both wings are presented in table I.

Two basic nacelle shapes were used during most of these tests. The open nacelle (fig. 2(a)) allowed straight-through air passage and the faired nacelle (fig. 2(b)) was closed at both entrance and exit. The three NACA series one-nose inlets (ref. 8) used on the open nacelle are illustrated in figure 2(a). Dimensions of both faired and open nacelles are given in figure 2.

The faired nacelles were mounted at four vertical positions with respect to the wing chord plane. The open nacelles were tested only at position 3 as shown in figure 3. The positions designations denoted in figure 3 will be used throughout this paper. The nacelles were supported on each wing panel by variable length struts which were swept forward  $75^\circ$ . The angle between the nacelle center line and the line formed by joining the top of the nacelle exit lip with the wing trailing edge at the nacelle station was constant at  $15^\circ$  for all open nacelles tested. Nacelle strut details are shown in figure 2.

The submerged nacelle installations which were tested on the 6-percent-thick and thickened root wings are shown in figures 4(a) and 4(b), respectively. The frontal areas (including the area buried in the wing) of two submerged nacelles and of one open or faired nacelle (fig. 3) were equal.

The models were sting-supported and had a six-component internal strain-gage balance in the body. The model and sting are shown in figure 5.

The models, balance, and indicating equipment were furnished by an Air Force contractor.

## TESTS, CORRECTIONS, AND ACCURACY

### Tests

The conditions for the tests of the wing-body configurations were:

|   |                   |
|---|-------------------|
| Mach number . . . . .                                 | 2.01              |
| Reynolds number, based on $\bar{c}$ . . . . .         | $2.2 \times 10^6$ |
| Stagnation dewpoint, $^\circ\text{F}$ . . . . .       | $<-30$            |
| Stagnation pressure, pounds per square inch . . . . . | 14                |
| Stagnation temperature, $^\circ\text{F}$ . . . . .    | 110               |

Tests of all configurations were made through an angle-of-attack range from  $-2^\circ$  to  $13^\circ$ . The body alone and the basic wing-body combination were tested with and without a transition strip on the nose to establish the type of boundary layer existing during the tests (ref. 6). The boundary layer of the body alone was laminar for the Reynolds number of the test. The nacelle configurations presented in this investigation were not tested with transition strips.

### Corrections and Accuracy

Calibration of the nozzle prior to these tests has shown that the flow in the test section is reasonably uniform. The magnitude of the variations in the flow parameters is summarized in the following table:

|   |             |
|---|-------------|
| Mach number . . . . .                               | $\pm 0.015$ |
| Flow angle in horizontal plane, degrees . . . . .   | $\pm 0.1$   |
| Flow angle in the vertical plane, degrees . . . . . | $\pm 0.1$   |

The angle of attack of the model was corrected for deflection of the balance and support system due to lift and pitching moment. Angle corrections were obtained from in-place calibration of the balance for various lift loads and pitching moments.

The validity of these corrections was verified during the tests at  $M = 1.60$  (ref. 3). The estimated angle-of-attack error was  $\pm 0.1^\circ$ . During these tests, the model was yawed about  $-0.2^\circ$  due to misalignment. No corrections were applied for this yaw angle or for the flow variation in the test section.

The estimated errors in the force data obtained by comparing the results of two tests of the same configurations are as follows:

|                 |             |
|-----------------|-------------|
| $C_L$ . . . . . | $\pm 0.001$ |
| $C_D$ . . . . . | $\pm 0.001$ |
| $C_m$ . . . . . | $\pm 0.001$ |

The base pressure for all configurations tested was measured and the drag data were corrected to correspond to a base pressure equal to free-stream static pressure.

### RESULTS

The results are presented in this paper with a minimum of analysis to expedite publication. The variations of drag, nacelle drag increment, pitching moment, and angle of attack with lift coefficient are presented in figures 6 to 10 for a Mach number of 2.01 and a Reynolds number of  $2.2 \times 10^6$  based on the wing mean aerodynamic chord. The factor required to convert the nacelle drag increment to a value based on nacelle frontal area is listed in each figure. A test with transition fixed at the nose of the body on the 6-percent-thick wing-body combination showed only a slight increase in drag (ref. 6).

The lift-drag ratios for most of the configurations are presented in figure 11. It is evident from figure 11 that the nacelle shape and location have only a small effect on the maximum lift-drag ratio. The drag penalty of the thickened root wing-body configuration becomes small when the use of simulated submerged nacelles is considered. Representative schlieren pictures are presented in figure 12.

In general, the magnitudes of the drag increment at  $M = 2.01$  are of the same order as the drag increments at  $M = 1.6$  (ref. 5). The maximum lift-drag ratios, however, decreased with increasing Mach numbers.

Langley Aeronautical Laboratory  
National Advisory Committee for Aeronautics  
Langley Field, Va.

## REFERENCES

1. Bielat, Ralph P., Harrison, Daniel E., and Coppolino, Domenic A.: An Investigation at Transonic Speeds of the Effects of Thickness Ratio and of Thickened Root Sections on the Aerodynamic Characteristics of Wings With  $47^\circ$  Sweepback, Aspect Ratio 3.5, and Taper Ratio 0.2 in the Slotted Test Section of the Langley 8-Foot High-Speed Tunnel. NACA RM L51I04a, 1951.
2. Bielat, Ralph P.: A Transonic Wind-Tunnel Investigation of the Aerodynamic Characteristics of Three 4-Percent-Thick Wings of Sweepback Angles  $10.8^\circ$ ,  $35^\circ$ , and  $47^\circ$ , Aspect Ratio 3.5, and Taper Ratio 0.2 in Combination With a Body. NACA RM L52B08, 1952.
3. Robinson, Ross B., and Driver, Cornelius: Aerodynamic Characteristics at Supersonic Speeds of a Series of Wing-Body Combinations Having Cambered Wings With an Aspect Ratio of 3.5 and a Taper Ratio of 0.2. Effects of Sweep Angle and Thickness Ratio on the Aerodynamic Characteristics in Pitch at  $M = 1.60$ . NACA RM L51K16a, 1952.
4. Spearman, M. Leroy, and Hilton, John H., Jr.: Aerodynamic Characteristics at Supersonic Speeds of a Series of Wing-Body Combinations Having Cambered Wings With an Aspect Ratio of 3.5 and a Taper Ratio of 0.2. Effects of Sweep Angle and Thickness Ratio on the Static Lateral Stability Characteristics at  $M = 1.60$ . NACA RM L51K15a, 1952.
5. Hasel, Lowell E., and Sevier, John R., Jr.: Aerodynamic Characteristics at Supersonic Speeds of a Series of Wing-Body Combinations Having Cambered Wings With an Aspect Ratio of 3.5 and a Taper Ratio of 0.2. Effect at  $M = 1.60$  of Nacelle Shape and Position on the Aerodynamic Characteristics in Pitch of Two Wing-Body Combinations with  $47^\circ$  Sweptback Wings. NACA RM L51K14a, 1952.
6. Robinson, Ross B.: Aerodynamic Characteristics at Supersonic Speeds of a Series of Wing-Body Combinations Having Cambered Wings With an Aspect Ratio of 3.5 and a Taper Ratio of 0.2. Effects of Sweep Angle and Thickness Ratio on the Aerodynamic Characteristics in Pitch at  $M = 2.01$ . NACA RM L52E09, 1952.
7. Hamilton, Clyde V.: Aerodynamic Characteristics at Supersonic Speeds of a Series of Wing-Body Combinations Having Cambered Wings with an Aspect Ratio of 3.5 and a Taper Ratio of 0.2. Effects of Sweep Angle and Thickness Ratio on the Static Lateral Stability Characteristics at  $M = 2.01$ . NACA RM L52E23, 1952.

8. Baals, Donald D., Smith, Norman F., and Wright, John B.: The Development and Application of High-Critical-Speeds Nose Inlets. NACA Rep. 920, 1948. (Supersedes NACA ACR L5F30a.)

TABLE I  
AIRFOIL COORDINATES FOR THE VARIOUS WINGS

 $\frac{t}{c} = 0.04$ 

| x/c                   | y/c<br>upper<br>surface | y/c<br>lower<br>surface |
|-----------------------|-------------------------|-------------------------|
| 0                     | 0                       | 0                       |
| .5                    | .411                    | .245                    |
| .75                   | .499                    | .271                    |
| 1.25                  | .665                    | .289                    |
| 2.5                   | .962                    | .324                    |
| 5.0                   | 1.435                   | .367                    |
| 7.5                   | 1.776                   | .429                    |
| 10                    | 2.039                   | .472                    |
| 15                    | 2.423                   | .577                    |
| 20                    | 2.642                   | .682                    |
| 25                    | 2.800                   | .787                    |
| 30                    | 2.887                   | .892                    |
| 35                    | 2.983                   | .997                    |
| 40                    | 2.992                   | 1.006                   |
| 45                    | 2.940                   | 1.041                   |
| 50                    | 2.852                   | 1.006                   |
| 55                    | 2.712                   | .945                    |
| 60                    | 2.511                   | .857                    |
| 65                    | 2.265                   | .761                    |
| 70                    | 1.986                   | .674                    |
| 75                    | 1.680                   | .577                    |
| 80                    | 1.356                   | .481                    |
| 85                    | 1.041                   | .385                    |
| 90                    | .726                    | .289                    |
| 95                    | .402                    | .201                    |
| 100                   | .105                    | .105                    |
| Tangent<br>point      | 80.00                   | 60.00                   |
| L.E. radius = 0.0016c |                         |                         |

 $\frac{t}{c} = 0.06$ 

| x/c                   | y/c<br>upper<br>surface | y/c<br>lower<br>surface |
|-----------------------|-------------------------|-------------------------|
| 0                     | 0.061                   | 0                       |
| .5                    | .577                    | .376                    |
| .75                   | .717                    | .446                    |
| 1.25                  | .919                    | .534                    |
| 2.5                   | 1.304                   | .621                    |
| 5.0                   | 1.872                   | .761                    |
| 7.5                   | 2.318                   | .857                    |
| 10                    | 2.668                   | .980                    |
| 15                    | 3.150                   | 1.269                   |
| 20                    | 3.482                   | 1.496                   |
| 25                    | 3.701                   | 1.697                   |
| 30                    | 3.858                   | 1.846                   |
| 35                    | 3.946                   | 1.960                   |
| 40                    | 3.981                   | 2.021                   |
| 45                    | 3.937                   | 2.030                   |
| 50                    | 3.823                   | 1.977                   |
| 55                    | 3.613                   | 1.872                   |
| 60                    | 3.342                   | 1.697                   |
| 65                    | 3.018                   | 1.487                   |
| 70                    | 2.651                   | 1.277                   |
| 75                    | 2.231                   | 1.059                   |
| 80                    | 1.785                   | .849                    |
| 85                    | 1.338                   | .639                    |
| 90                    | .892                    | .420                    |
| 95                    | .446                    | .210                    |
| 100                   | 0                       | 0                       |
| L.E. radius = 0.0024c |                         |                         |

 $\frac{t}{c} = 0.09$ 

| x/c                   | y/c<br>upper<br>surface | y/c<br>lower<br>surface |
|-----------------------|-------------------------|-------------------------|
| 0                     | 0.156                   | 0                       |
| .5                    | .846                    | .574                    |
| .75                   | 1.021                   | .680                    |
| 1.25                  | 1.283                   | .846                    |
| 2.5                   | 1.789                   | 1.069                   |
| 5.0                   | 2.537                   | 1.400                   |
| 7.5                   | 3.111                   | 1.662                   |
| 10                    | 3.577                   | 1.896                   |
| 15                    | 4.244                   | 2.352                   |
| 20                    | 4.705                   | 2.751                   |
| 25                    | 5.045                   | 3.052                   |
| 30                    | 5.288                   | 3.276                   |
| 35                    | 5.415                   | 3.441                   |
| 40                    | 5.473                   | 3.529                   |
| 45                    | 5.424                   | 3.519                   |
| 50                    | 5.249                   | 3.422                   |
| 55                    | 4.967                   | 3.208                   |
| 60                    | 4.579                   | 2.916                   |
| 65                    | 4.102                   | 2.566                   |
| 70                    | 3.568                   | 2.197                   |
| 75                    | 2.975                   | 1.837                   |
| 80                    | 2.382                   | 1.468                   |
| 85                    | 1.789                   | 1.098                   |
| 90                    | 1.186                   | .739                    |
| 95                    | .593                    | .369                    |
| 100                   | 0                       | 0                       |
| L.E. radius = 0.0056c |                         |                         |

Thickened root

| x/c                   | Root station            |                         |
|-----------------------|-------------------------|-------------------------|
|                       | y/c<br>upper<br>surface | y/c<br>lower<br>surface |
| 0                     | 0.301                   | 0                       |
| .5                    | 1.120                   | .754                    |
| .75                   | 1.335                   | .904                    |
| 1.25                  | 1.658                   | 1.141                   |
| 2.5                   | 2.261                   | 1.507                   |
| 5.0                   | 3.208                   | 2.024                   |
| 7.5                   | 3.919                   | 2.433                   |
| 10                    | 4.500                   | 2.799                   |
| 15                    | 5.362                   | 3.445                   |
| 20                    | 5.965                   | 3.984                   |
| 25                    | 6.395                   | 4.414                   |
| 30                    | 6.718                   | 4.716                   |
| 35                    | 6.912                   | 4.910                   |
| 40                    | 6.977                   | 5.017                   |
| 45                    | 6.912                   | 4.996                   |
| 50                    | 6.675                   | 4.823                   |
| 55                    | 6.288                   | 4.522                   |
| 60                    | 5.771                   | 4.113                   |
| 65                    | 5.168                   | 3.618                   |
| 70                    | 4.457                   | 3.101                   |
| 75                    | 3.725                   | 2.584                   |
| 80                    | 2.929                   | 2.067                   |
| 85                    | 2.239                   | 1.550                   |
| 90                    | 1.486                   | 1.034                   |
| 95                    | .732                    | .517                    |
| 100                   | 0                       | 0                       |
| L.E. radius = 0.0099c |                         |                         |

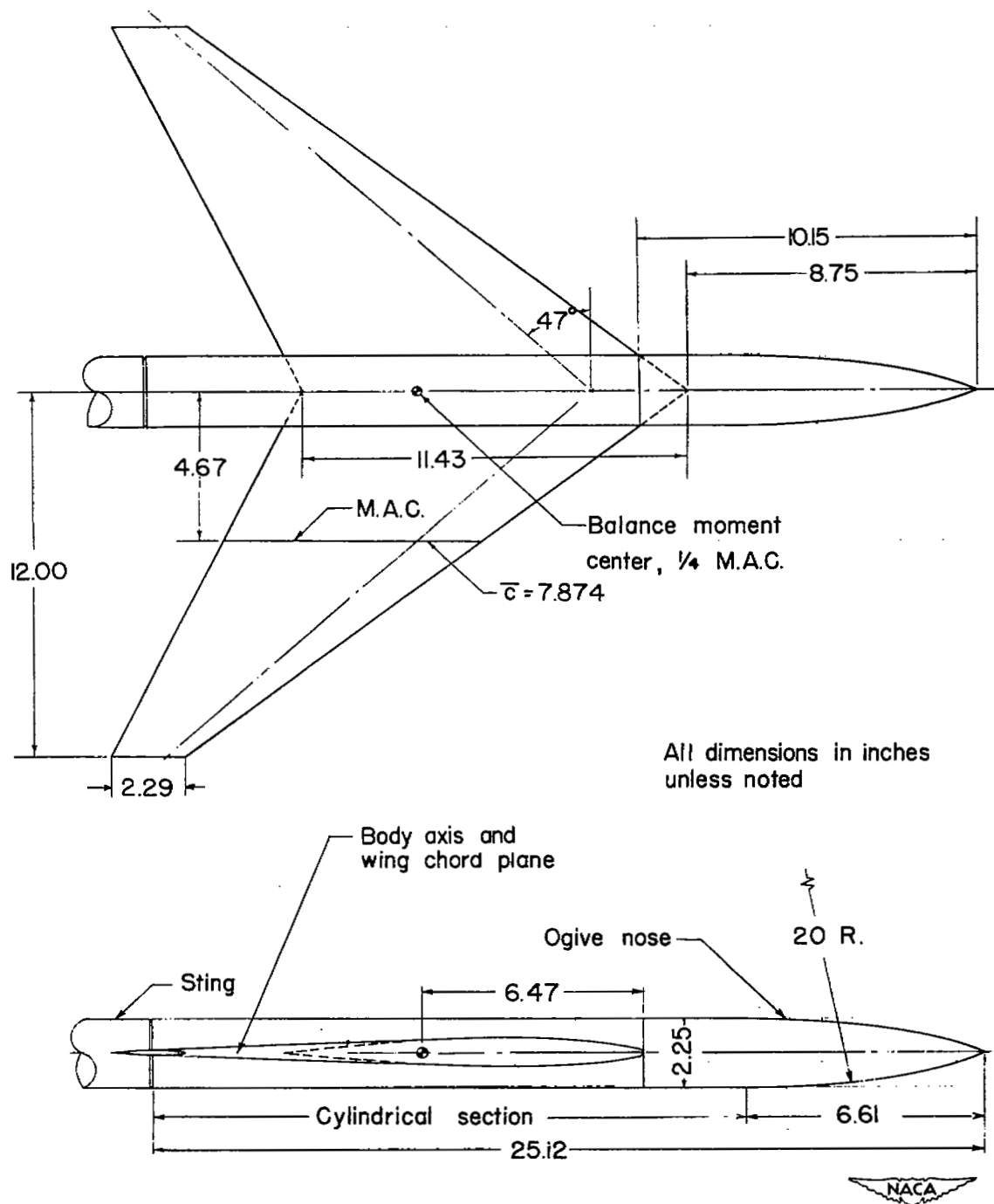
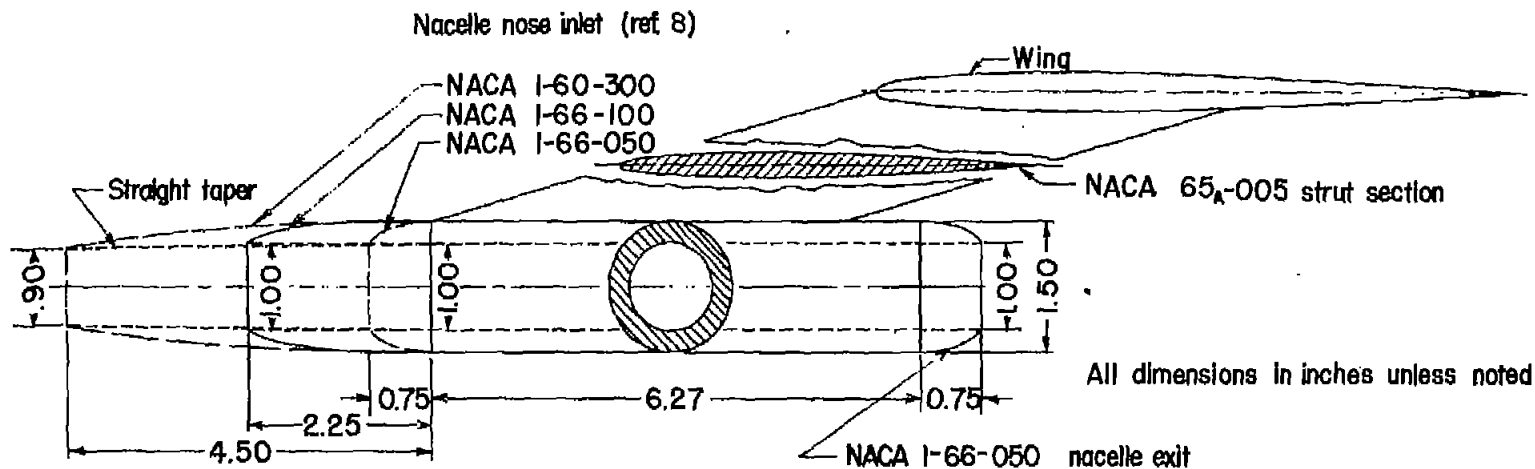
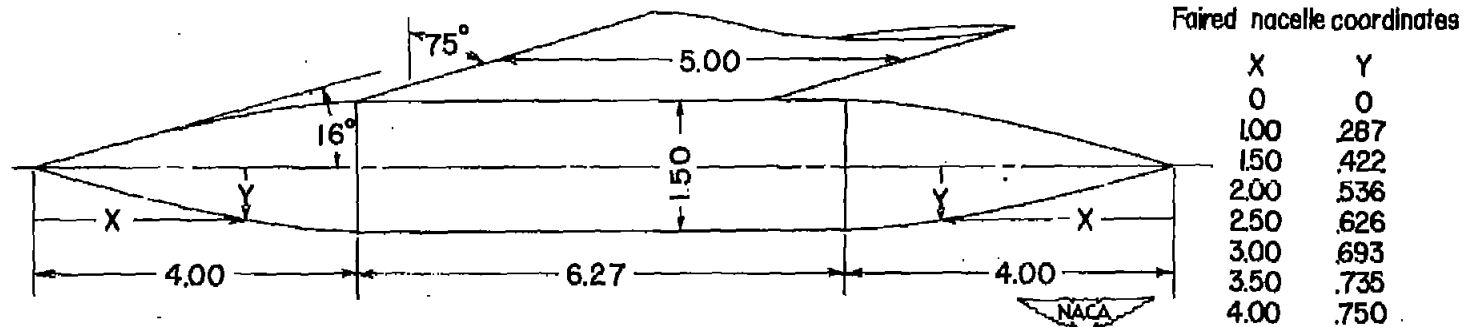


Figure 1.- Details of body and 47° sweptback wing.



(a) Open nacelles.



(b) Faired nacelle.

Figure 2.- Details of open and faired nacelles, and nacelle strut.

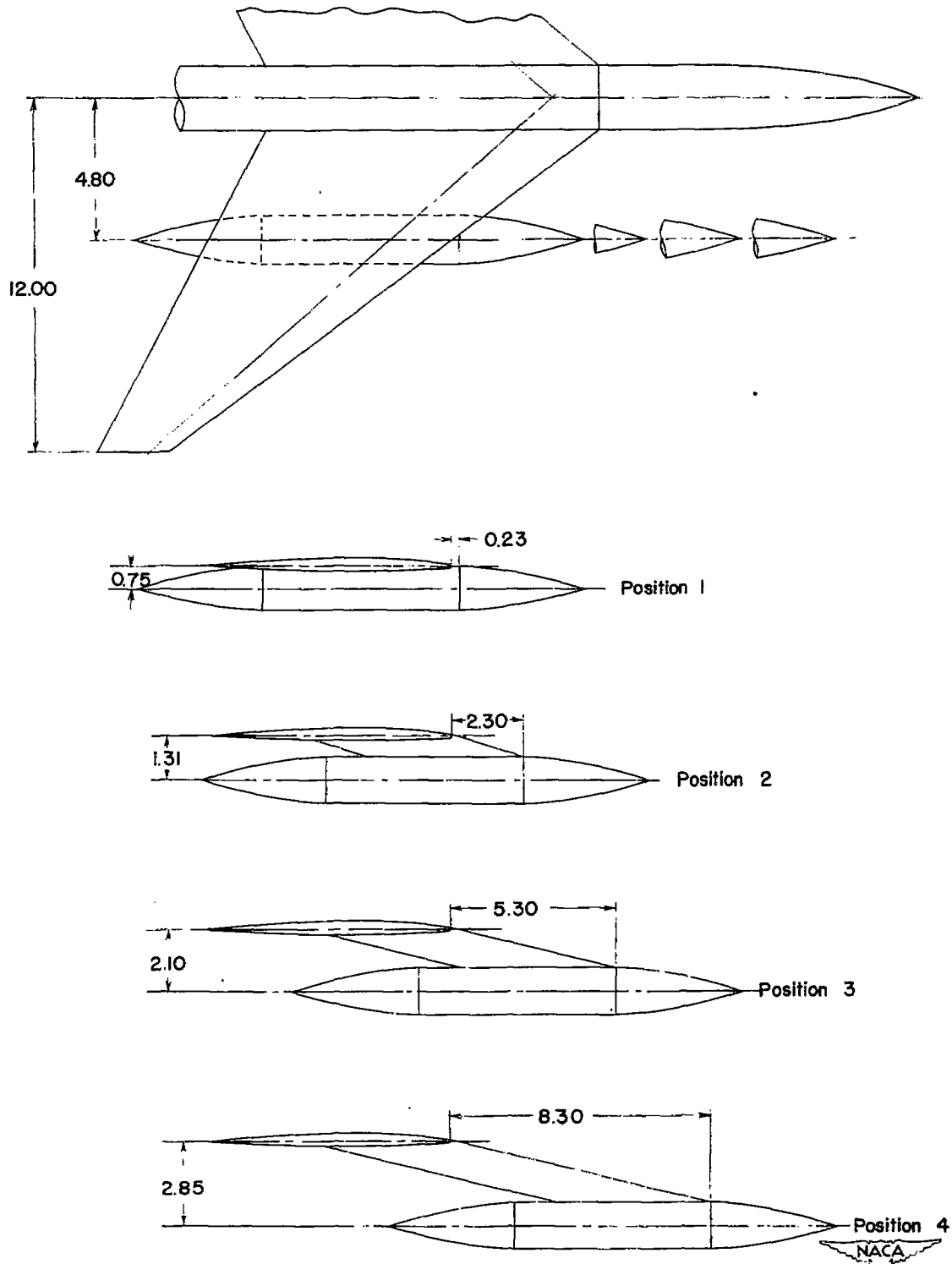
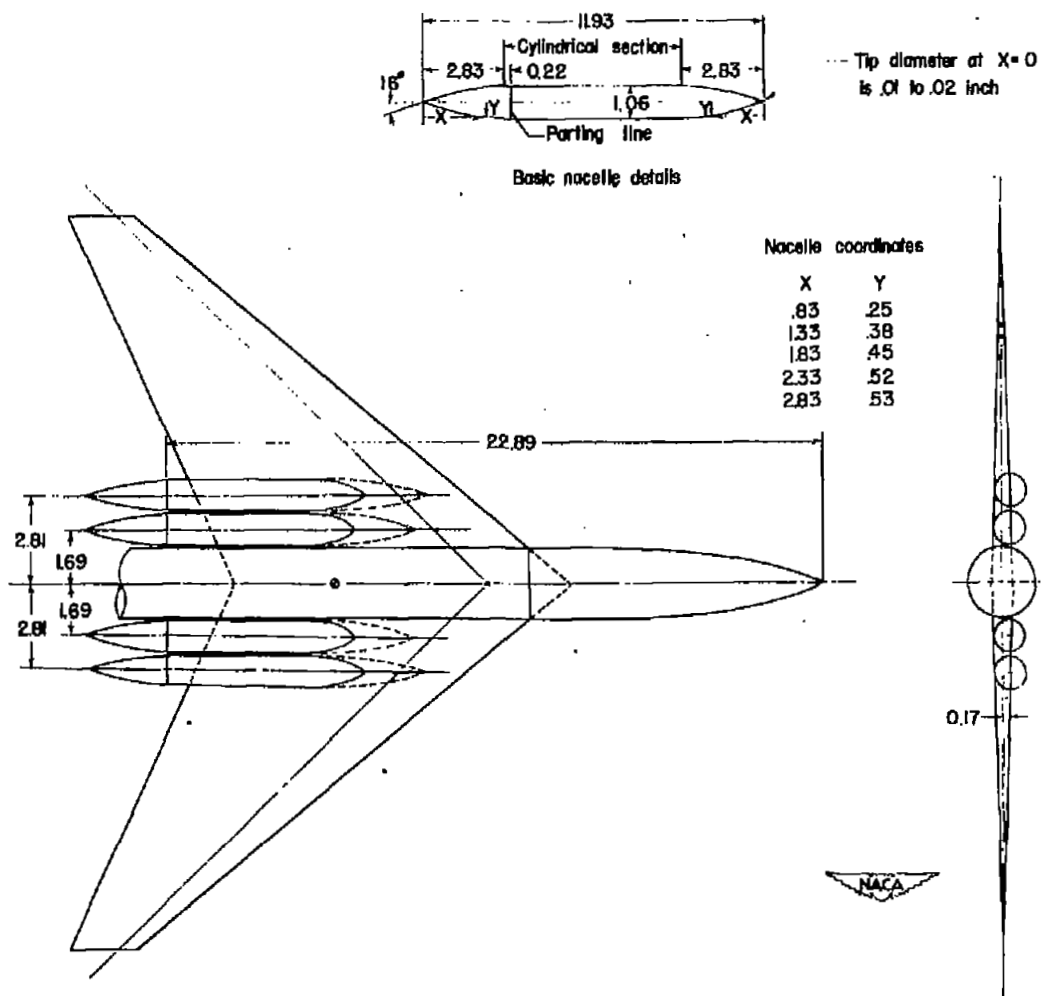
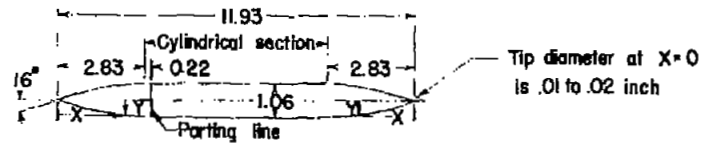


Figure 3.- Nacelle position designation.

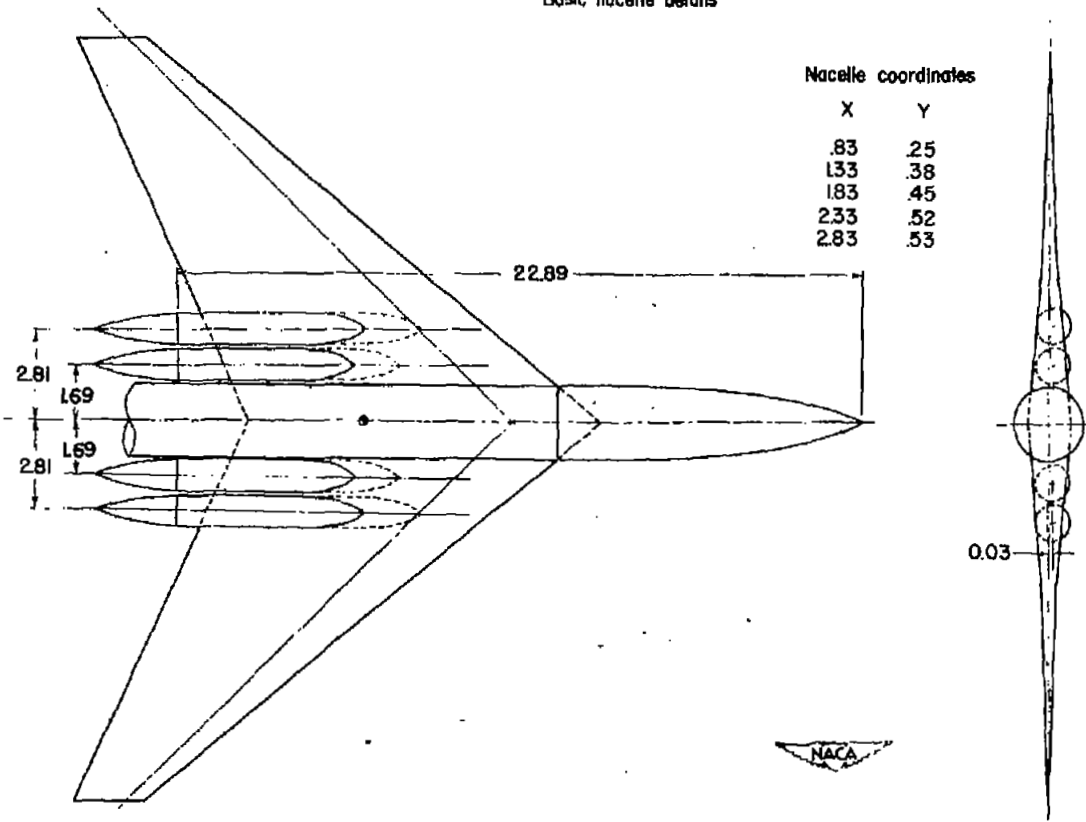


(a) Six-percent-thick wing.

Figure 4.- Details of submerged nacelles and nacelle locations on wings.  
All dimensions in inches unless noted.

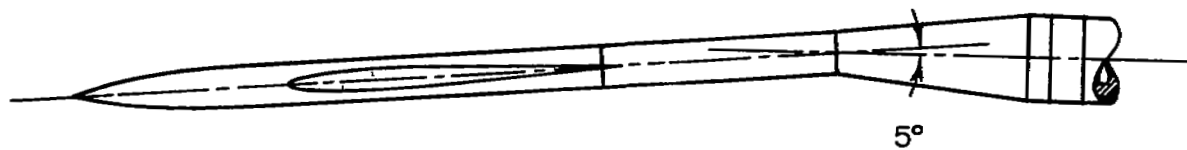


Basic nacelle details

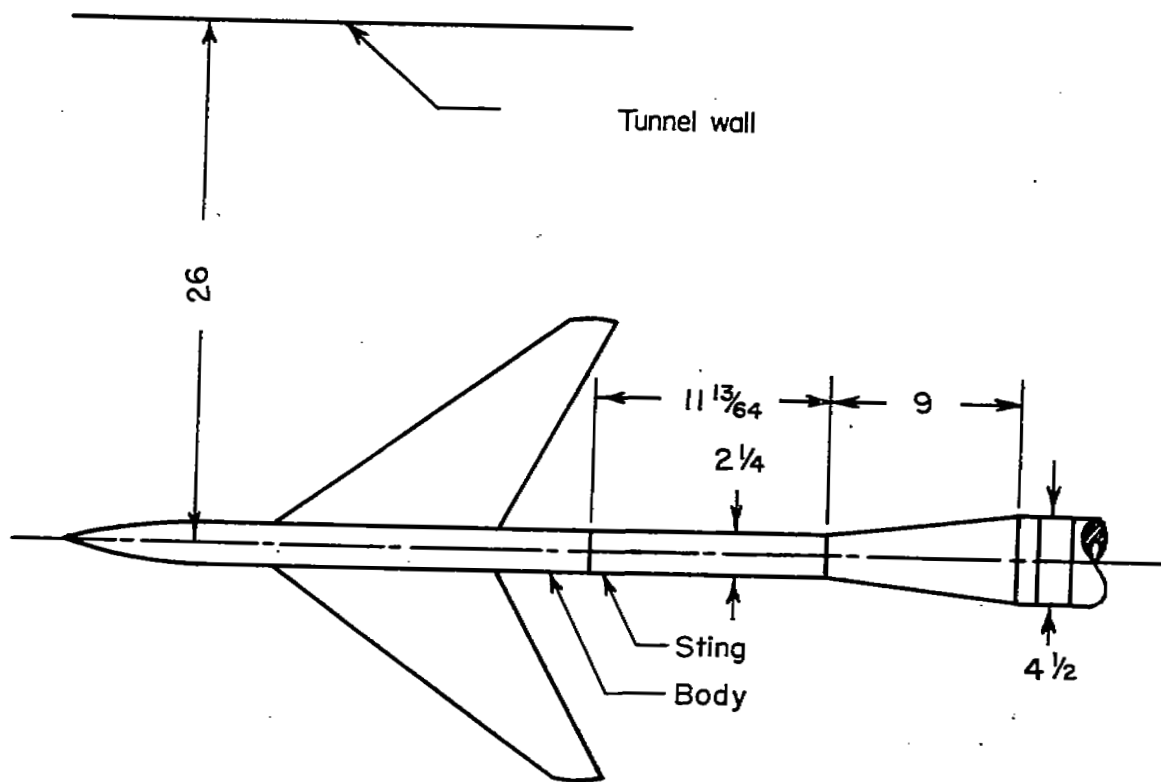


(b) Varying-thickness-ratio wing.

Figure 4.- Concluded.



Top view of installation



Side view of installation



Figure 5.- Details of model sting support. All dimensions in inches unless noted.

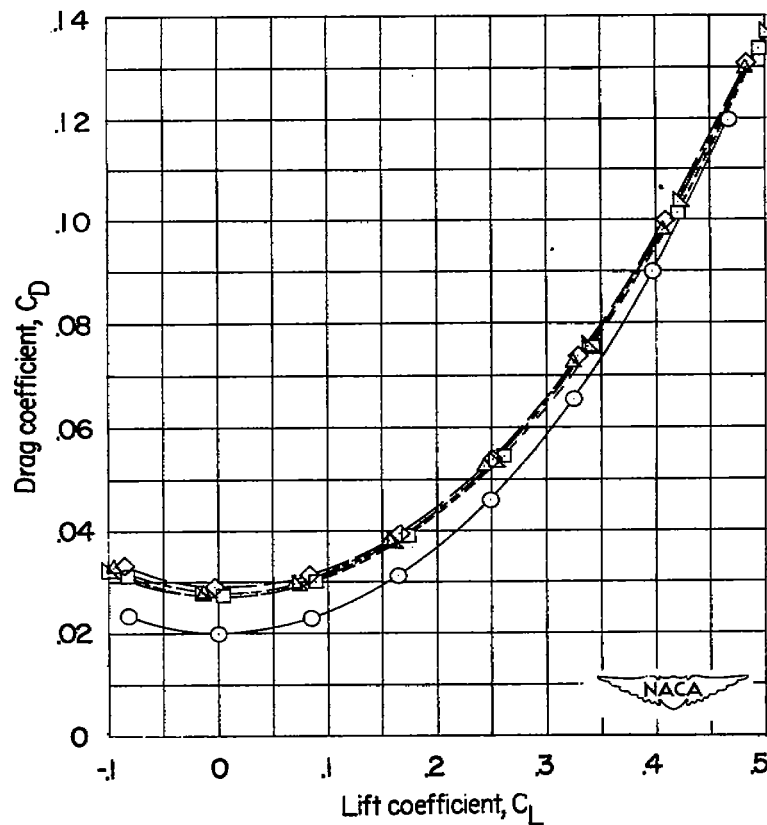
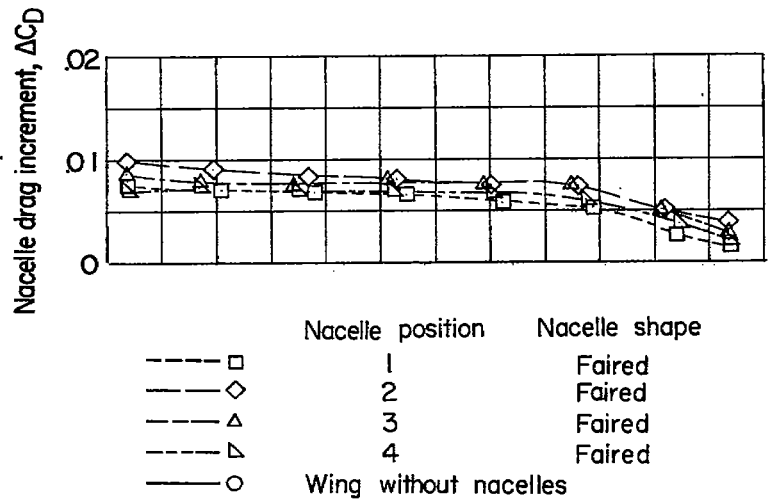


Figure 6.- Effect of position of strut-mounted faired nacelles on the longitudinal characteristics of the 6-percent-thick wing at  $M = 2.01$ . The ratio of wing-plan-form area to frontal area of the two nacelles is 46.57.

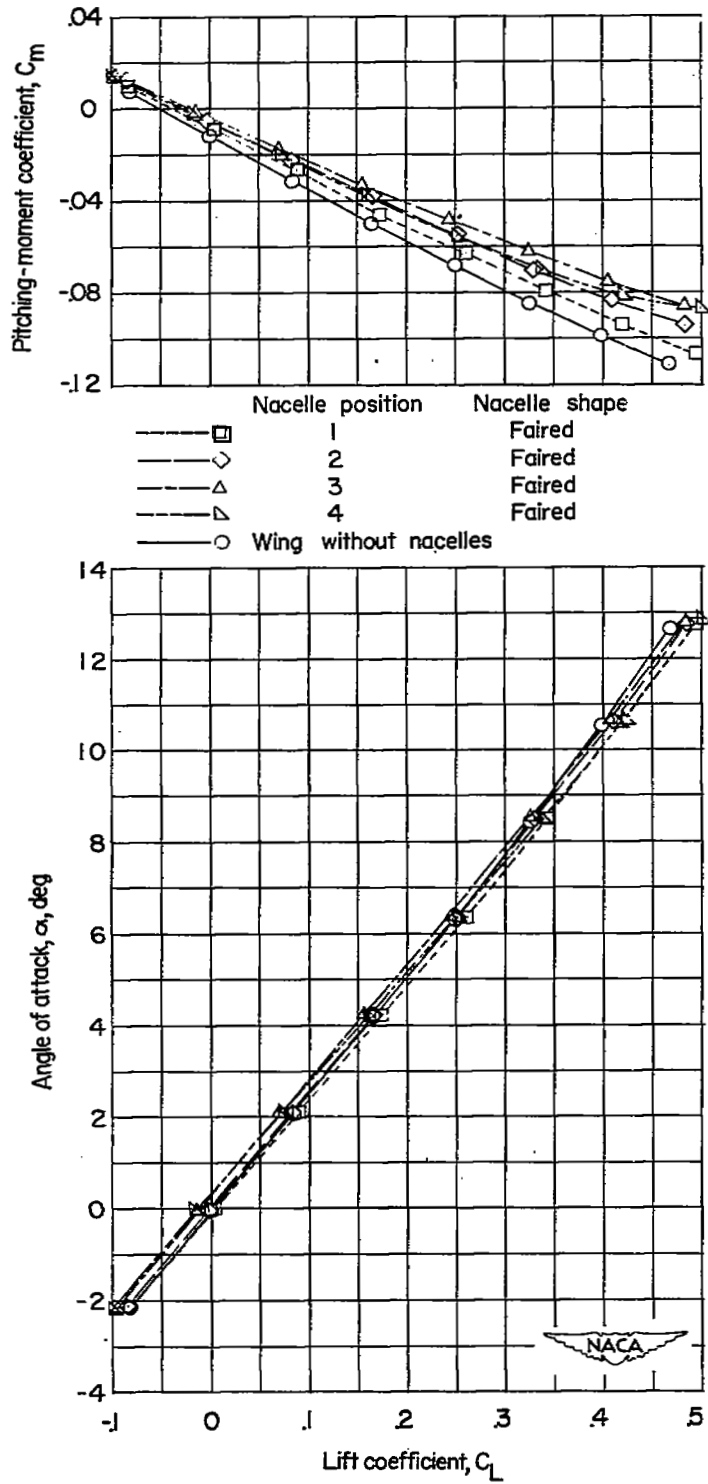


Figure 6.- Concluded.

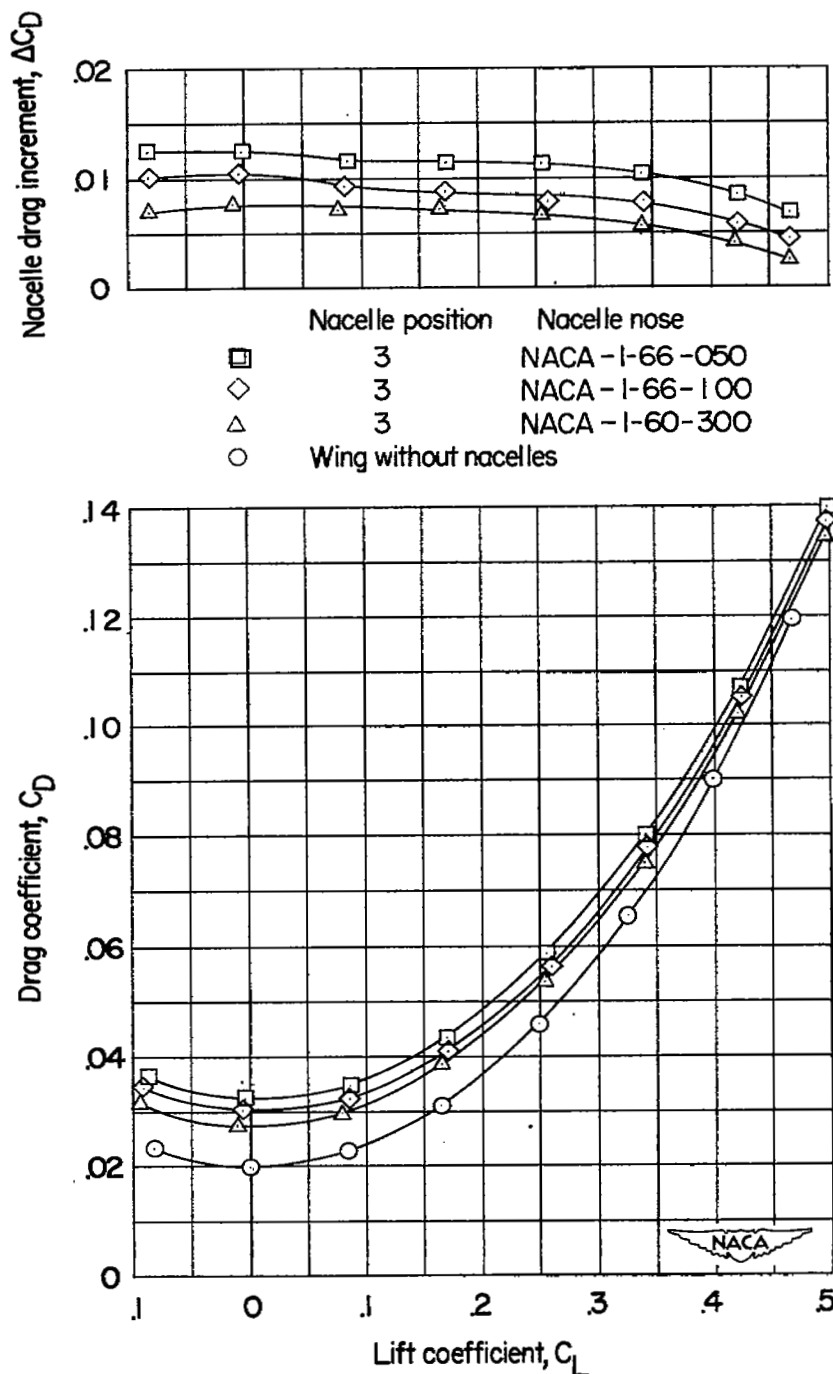
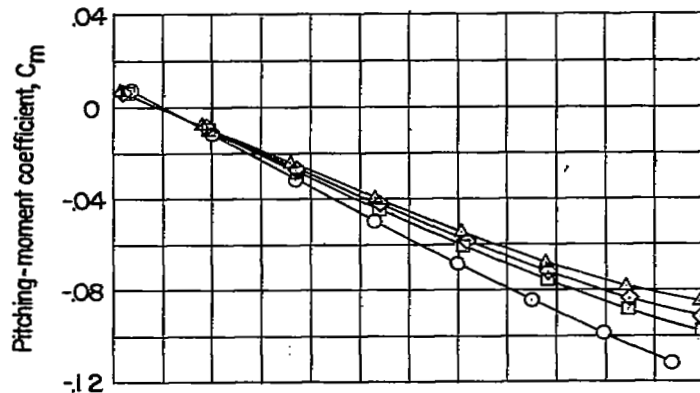


Figure 7.- The effect of various nose configurations on the longitudinal characteristics of the 6-percent-thick wing with the nacelles mounted at position 3 for  $M = 2.01$ . The ratio of wing-plan-form area to the frontal area of the two nacelles is 46.57.



|   | Nacelle position      | Nacelle nose   |
|---|-----------------------|----------------|
| □ | 3                     | NACA -1-66-050 |
| ◇ | 3                     | NACA -1-66-100 |
| △ | 3                     | NACA -1-60-300 |
| ○ | Wing without nacelles |                |

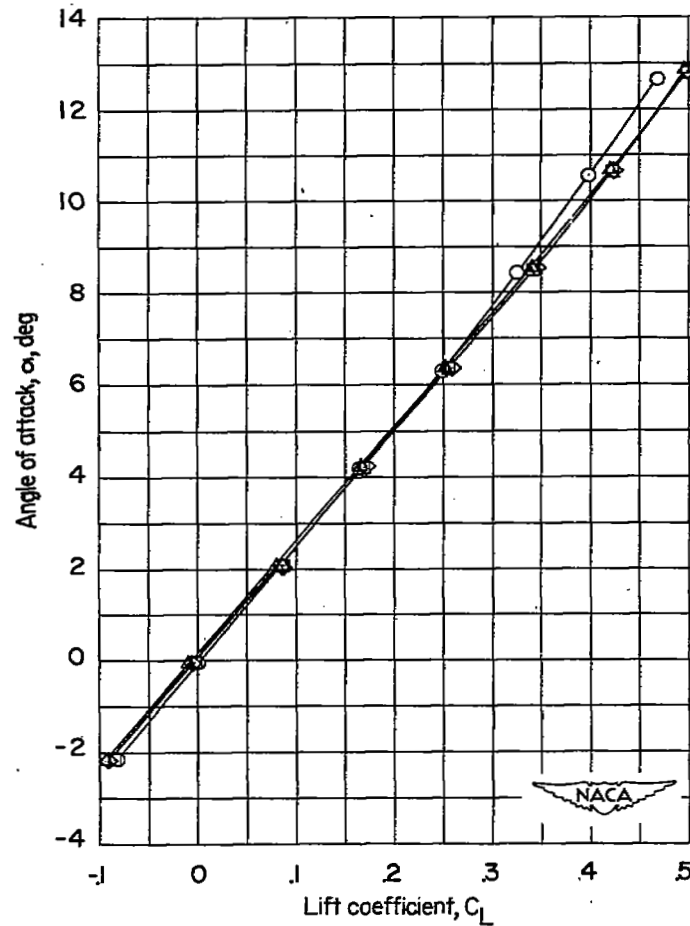


Figure 7.- Concluded.

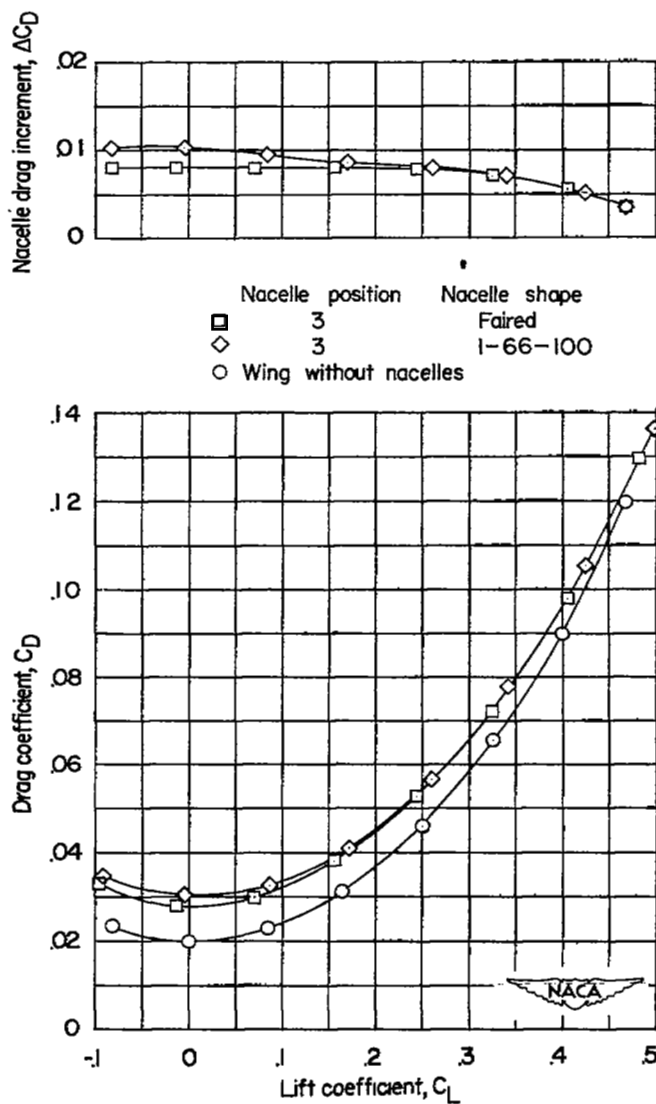
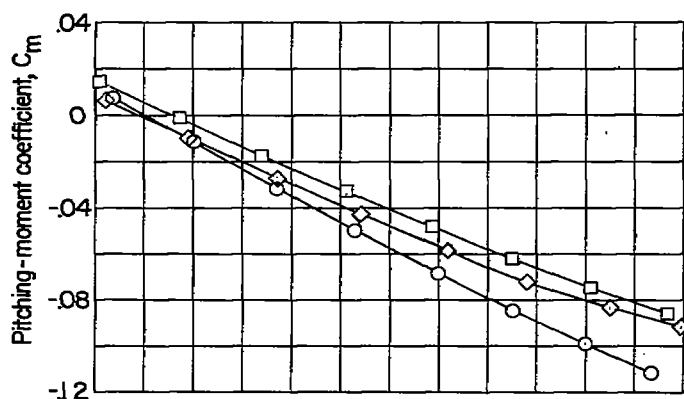


Figure 8.- Effect of nacelle shape on the longitudinal characteristics of the 6-percent-thick wing with the nacelle mounted at position 3 for  $M = 2.01$ . The ratio of wing-plan-form area to the frontal area of the two nacelles is 46.57.



|                  |                       |
|------------------|-----------------------|
| Nacelle position | Nacelle shape         |
| □ 3              | Faired                |
| ◇ 3              | NACA 1-66-100         |
| ○                | Wing without nacelles |

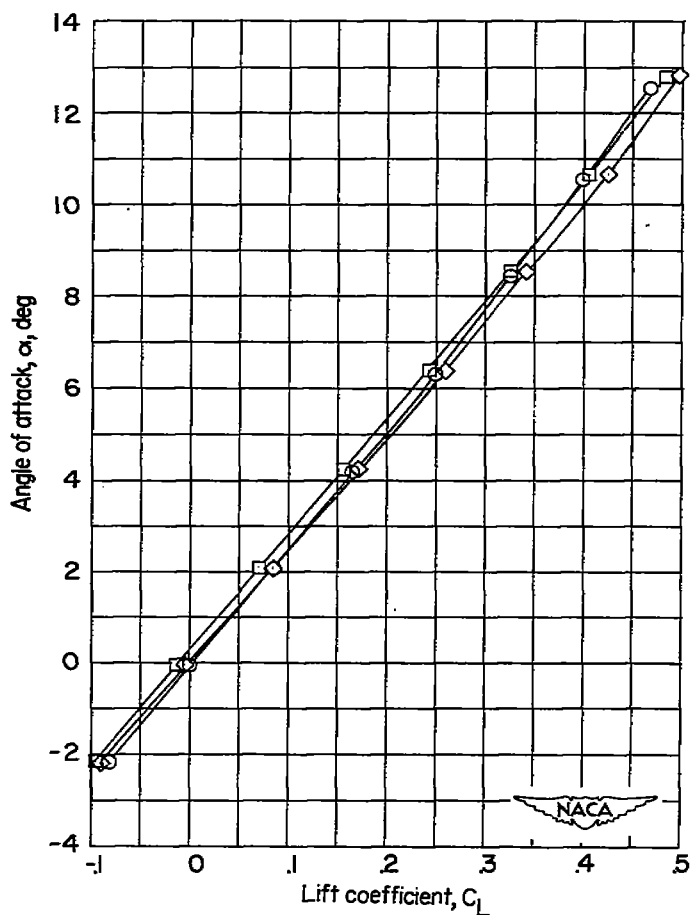


Figure 8.- Concluded.

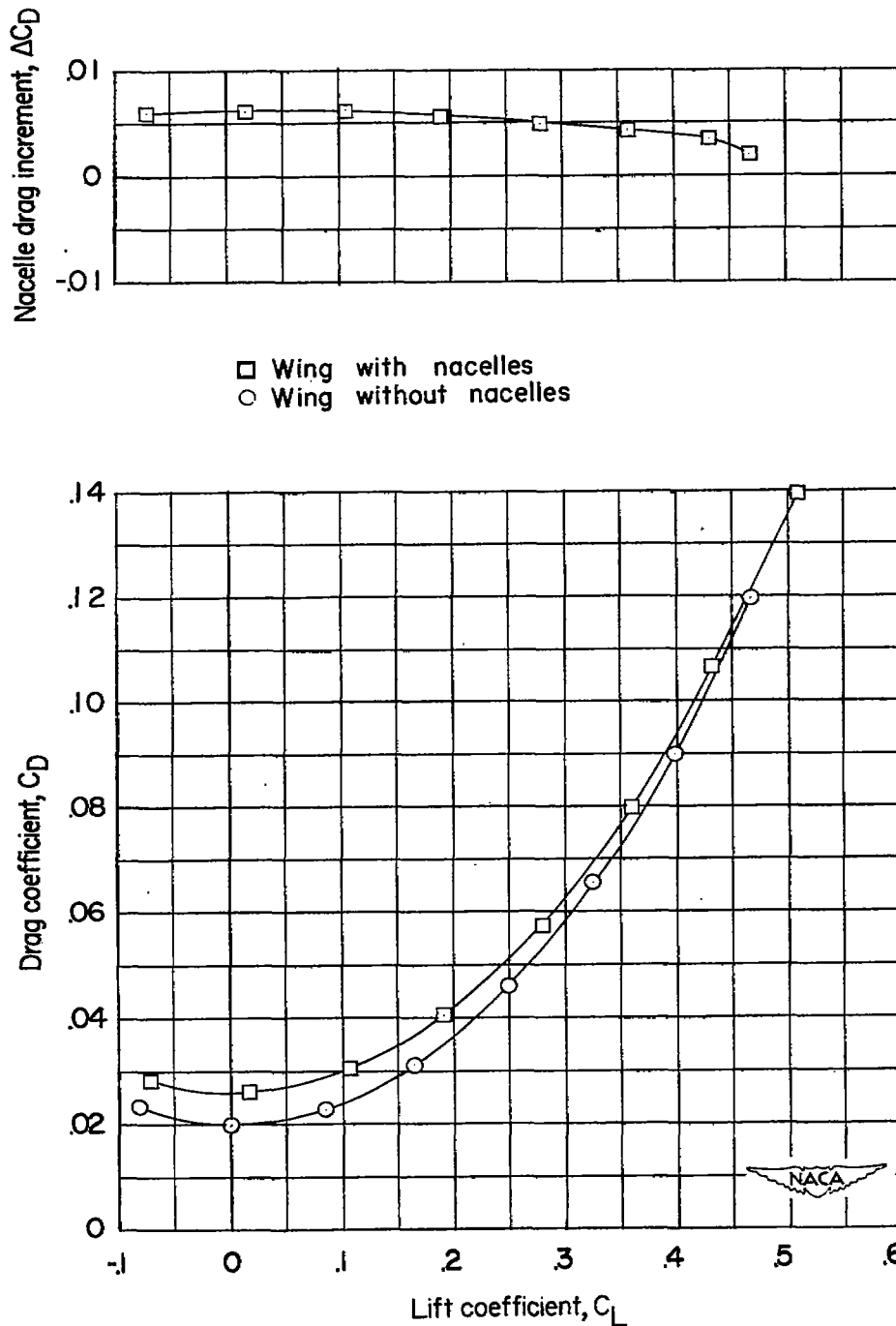


Figure 9.- Effect of faired submerged nacelles on the longitudinal characteristics of the 6-percent-thick wing at  $M = 2.01$ . The ratio of wing-plan-form area to the frontal area of the four nacelles is 46.63.

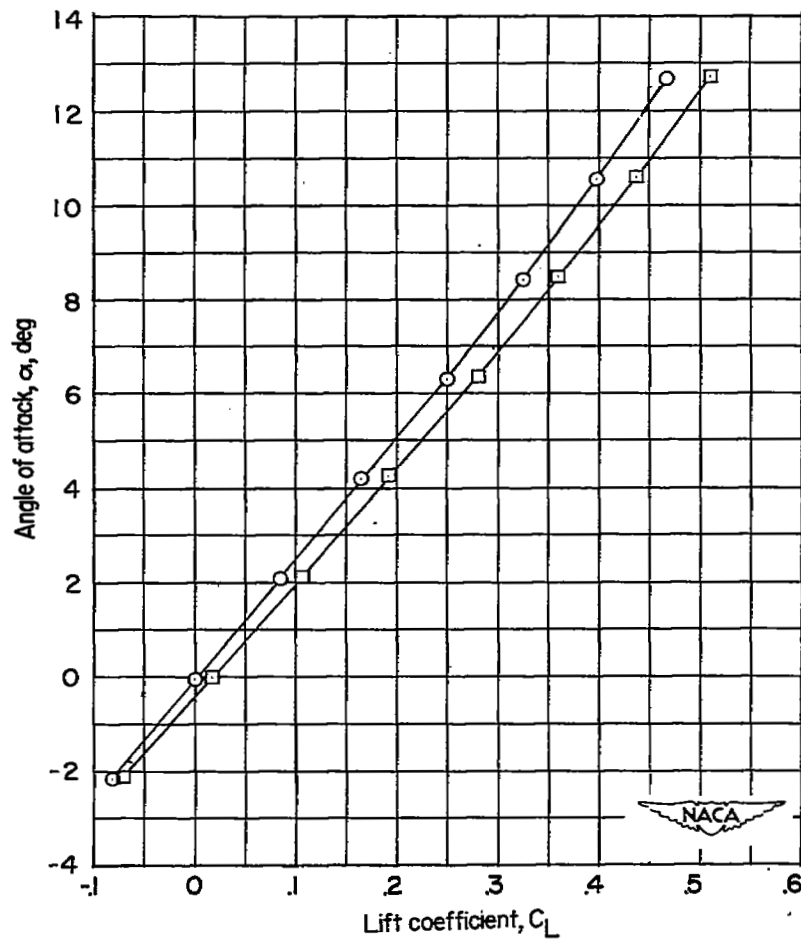
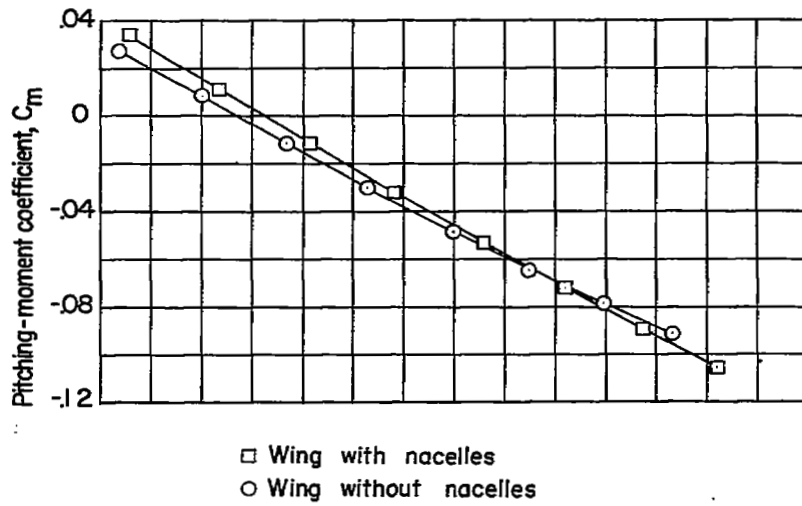


Figure 9.- Concluded.

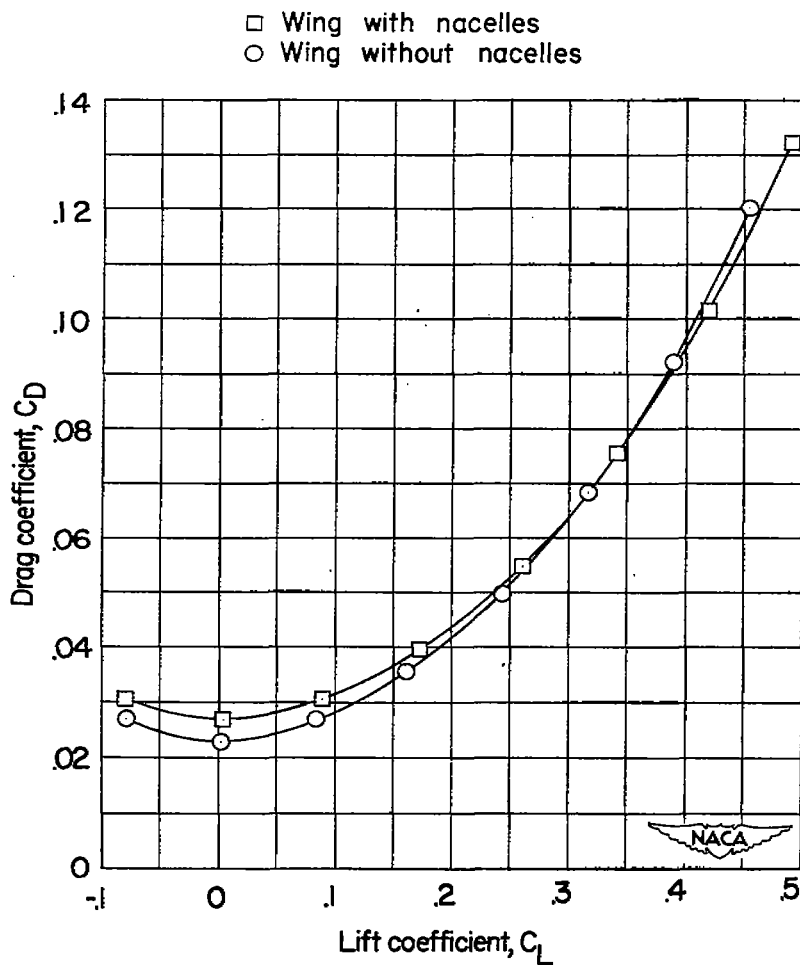
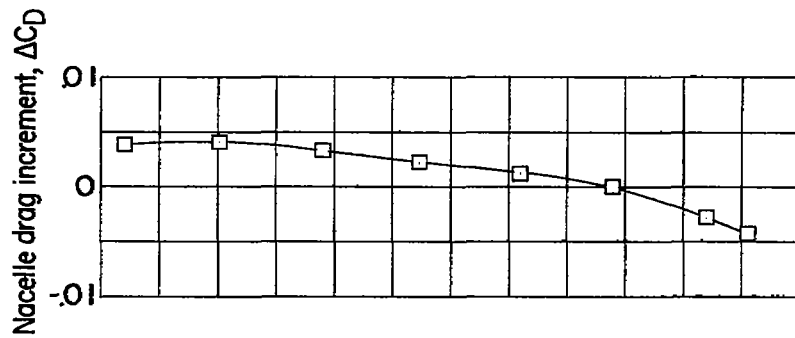
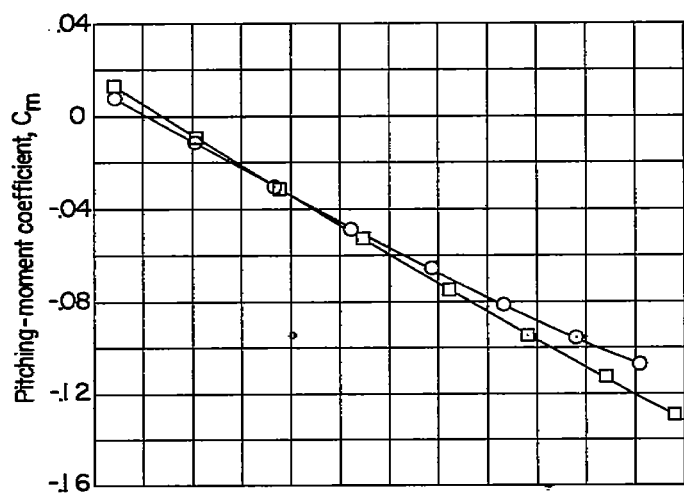


Figure 10.- Effect of faired submerged nacelles on the longitudinal characteristics of the wing with thickness ratio varying from 12 to 6 percent at  $M = 2.01$ . The ratio of wing-plan-form area to frontal area of the four nacelles is 46.63.



□ Wing with nacelles  
○ Wing without nacelles

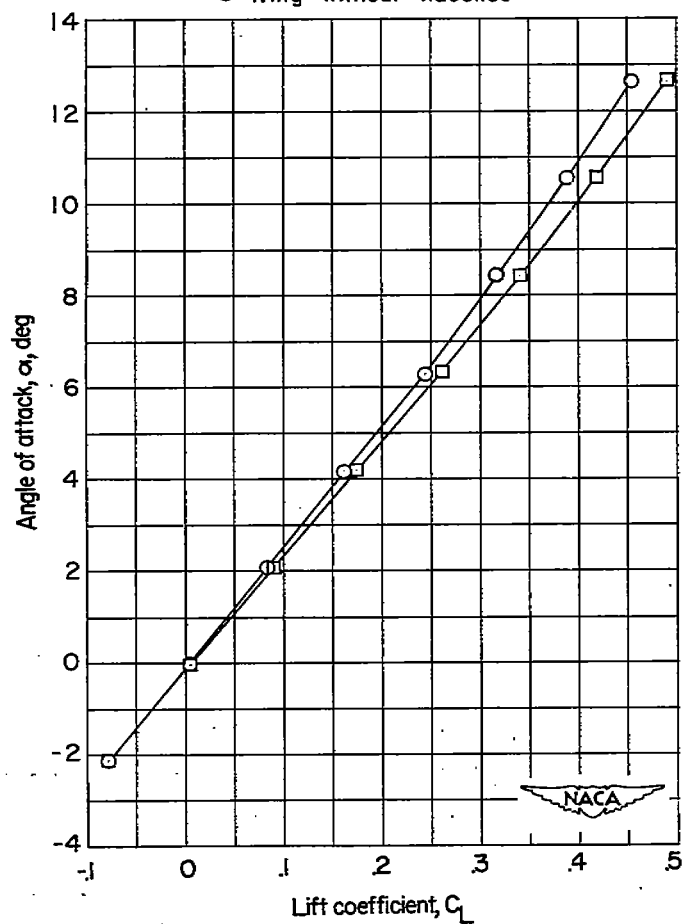


Figure 10.- Concluded.

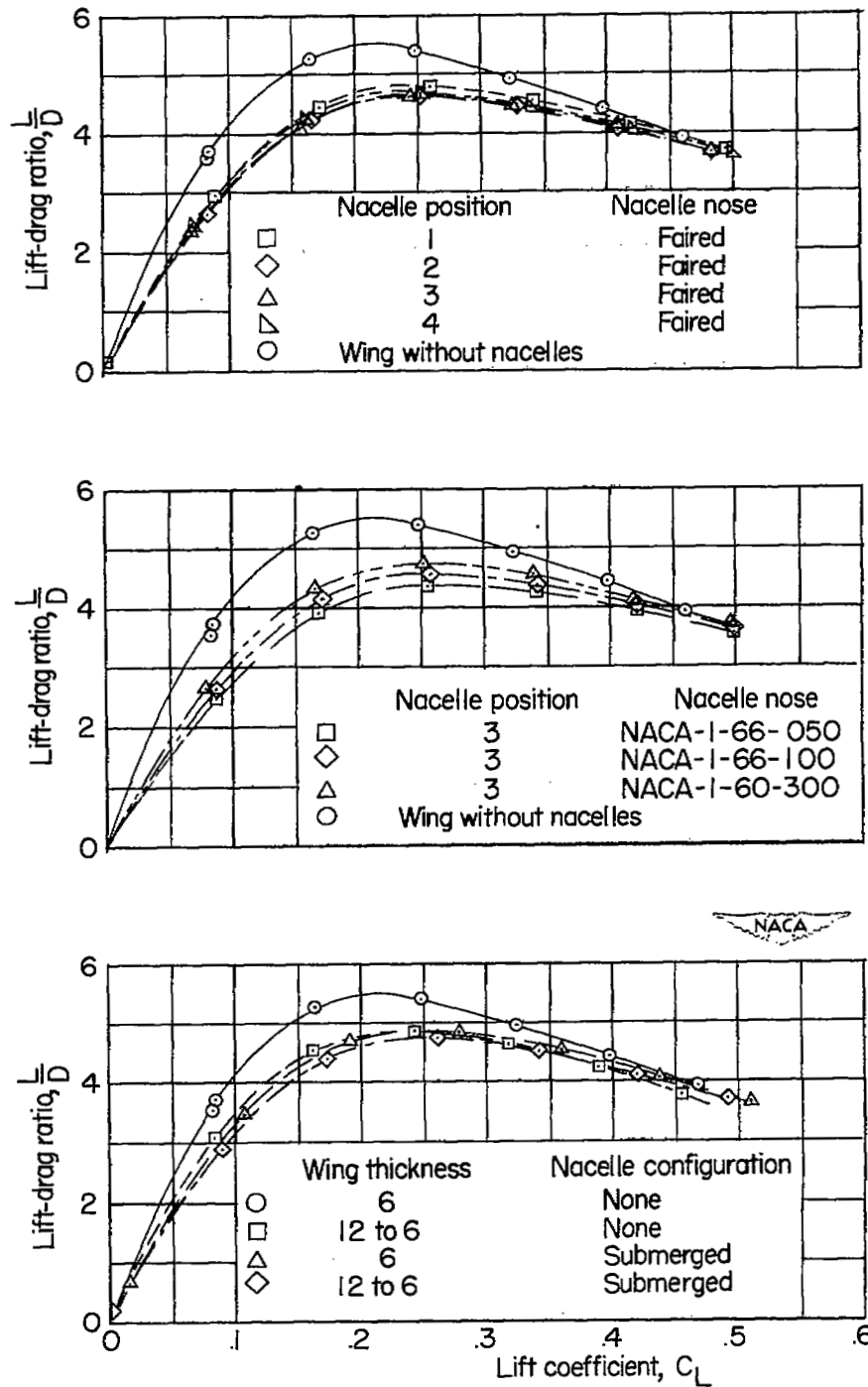
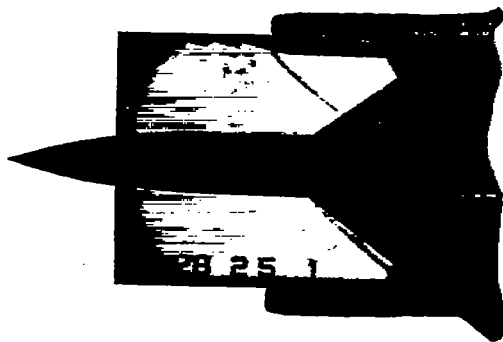
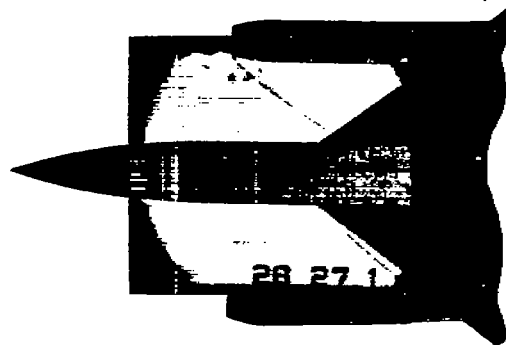


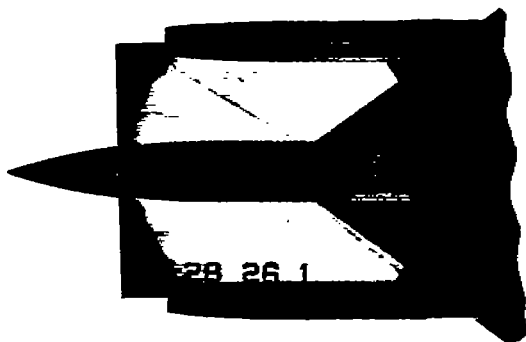
Figure 11.- Variation with lift coefficient of the lift-drag ratios of the 6-percent-thick and variable-thickness wings with and without nacelles.  $M = 2.01$ .



(a) NACA 1-66-050 nose inlet;  
 $\psi = 0^\circ$ .



(b) NACA 1-66-100 nose inlet;  
 $\psi = 0^\circ$ .



(c) NACA 1-60-300 nose inlet;  
 $\psi = 0^\circ$ .



(d) NACA 1-66-100 nose inlet;  
 $\psi = 5^\circ$ .

  
L-75113

Figure 12.- Schlieren photographs of open and faired nacelles mounted at position 3 on the 6-percent-thick wing.  $\alpha = 0^\circ$ ;  $M = 2.01$ .

**SECURITY INFORMATION**

NASA Technical Library



3 1176 01436 4781

2:

